PERGAMON

Solid State Communications 121 (2002) 531–536

solid state communications

www.elsevier.com/locate/ssc

Preferred orientation of ZnO nanoparticles formed by post-thermal annealing zinc implanted silica

Y.X. Liu[a], Y.C. Liu[a,b,*], D.Z. Shen[a], G.Z. Zhong[a], X.W. Fan[a], X.G. Kong[a], R. Mu[c], D.O. Henderson[c]

[a]*Open Laboratory of Excited State Processes, Changchun Institute of Optics, Fine Mechanics and Physics, Chinese Academy of Science, Changchun 130021, People's Republic of China*

[b]*The Institute of Theoretical Physics, Northeast Normal University, Changchun 130024, People's Republic of China*

[c]*Chemical Physics Laboratory, Department of Physics, Fisk University, Nashville, TN 37208, USA*

Received 5 November 2001; accepted 22 December 2001 by E. Molinari

Abstract

High quality zinc oxide nanoparticles with (002) preferred orientation were prepared by post-thermal annealing zinc implanted silica at 700 °C using two methods. One method was annealing zinc implanted silica at 700 °C for 2 h in oxygen ambient; the other method was sequentially annealing zinc implanted silica at 700 °C in nitrogen and oxygen ambient for 1 h, respectively. X-ray diffraction (XRD), absorption and microphotoluminescence (micro-PL) results indicated that the latter method could create high quality ZnO nanoparticles with (002) preferred orientation and narrow size-distribution. X-ray photoelectron spectra (XPS) showed the formation of ZnO nanoparticles on a silica surface, where the ZnO nanoparticle content increased with increasing oxidation time in an oxygen environment. The processes of the transformation from Zn to ZnO are discussed. © 2002 Elsevier Science Ltd. All rights reserved.

PACS: 78.66.Hf; 78.40.Fy; 61.14.Qp; 61.10.Kw; 78.55.−m

Keywords: ZnO; X-ray diffraction; X-ray photoelectron spectra; Annealing; Photoluminescence

1. Introduction

ZnO is a versatile semiconductor material with a wide band gap of 3.37 eV at room temperature. It has found application in piezoelectric and optoelectronic devices [1,2]. To obtain good piezoelectric activity and room temperature lasing, ZnO films should have perfect *c*-axis texture and narrow size-distribution of ZnO nanoparticles [3,4]. Many different techniques such as molecular beam epitaxy (MBE) [5], metal organic chemical vapor deposition (MOCVD) [6], pulse laser deposition [7], sputtering [8] and spray pyrolysis [9] have been used to prepare ZnO films with preferred orientation. Unfortunately, the use of many reactive sources for the preparation of ZnO can give rise to the impurities. Recently, Cho et al. reported a simple method for preparing polycrystalline ZnO thin film by the thermal oxidation of metallic Zn films [10], however, they could not obtain (002) preferred orientation ZnO. Therefore, it is imperative to find a simple and clean method to prepare ZnO film with preferred orientation.

Ion implantation is considered as one of the most clean and flexible technique to obtain nanoparticles [11]. In this article, an effort is made to use ion implantation as a tool to inject a low melting metal, Zn, into an optical-grade fused silica. Then Zn-implanted silica is thermally annealed in oxygen or nitrogen to obtain (002) preferred orientation ZnO nanoparticles on the silica surface. X-ray diffraction (XRD) and absorption data were used to characterize the formation of ZnO nanoparticles. X-ray photoelectron spectra (XPS) were used to investigate the thermal diffusion, effusion and oxidation processes of metallic Zn during the

* Corresponding author. Address: Open Laboratory of Excited State Processes, Changchun Institute of Optics, Fine Mechanics and Physics, Chinese Academy of Science, Changchun, 130021, People's Republic of China. Tel.: +86-431-5937596; fax: +86-431-5955378.

E-mail address: ycliu@nenu.edu.cn (Y.C. Liu).

0038-1098/02/$ - see front matter © 2002 Elsevier Science Ltd. All rights reserved.
PII: S0038-1098(02)00006-6

Table 1
The annealing condition of the samples

Sample	Annealing temperature	Ambient	Annealing time
IM4	As-implanted	–	–
IM5	700 °C	O_2	1 h
IM6	700 °C	O_2	2 h
IM7	700 °C	First N_2 then O_2	First 1 h then 1 h

annealing procedure as the annealing time and ambient changes. As far as we know, this is the first report to use ion implantation to obtain (002) preferred orientation ZnO nanoparticles under suitable annealing conditions. In our opinion, ion implantation may become a good method to prepare ZnO random laser, due to its ability to form high quality ZnO nanoparticles with preferred orientation on a silica surface.

2. Experiment

Optical-grade fused silica (Corning 7940) was used as the host material. Zn ions with an energy of 160 keV were injected into the substrate. The dose of implanted Zn was 3×10^{17} cm^{-2}. Based on Rutherford back scattering (RBS) measurements followed by the transport of ions in matter (TRIM) simulation, the Zn ion distribution in the silica substrate forms a nearly perfect Gaussian shape with the peak position at (0.12 ±0.01) μm below the surface. After ion implantation, the samples were annealed in a standard furnace using a quartz tube reactor. Samples were treated at 700 °C for 1 or 2 h in oxygen or nitrogen at atmospheric pressure, as given in Table 1.

The samples were characterized by means of XRD (D/max-rA Rigoku using Cu Kα, $\lambda = 1.5418$ Å) and absorption spectroscopy using UV360 spectrophotometer. The microphotoluminescence (micro-PL) of the ZnO nanocrystalline films was recorded using a JY UV-Lamb micro-Raman spectrometer in back scattering geometry configuration at room temperature. The excitation wavelength was 325 nm line of a He–Cd laser. The excitation area and power were 6 μm^2 and 45 MW, respectively. XPS were used to determine the chemical bonding configurations. XPS data were recorded at around 1×10^{-8} Torr using a VG ESCALAB MKIIsystem. To obtain binding energies of the constituent elements, a binding energy of 284.6 eV for a C1s line from the residual carbon on the surface was used as a reference.

3. Results and discussion

Fig. 1 shows θ–2θ XRD patterns of zinc implanted silica annealed at 700 °C under different annealing conditions.

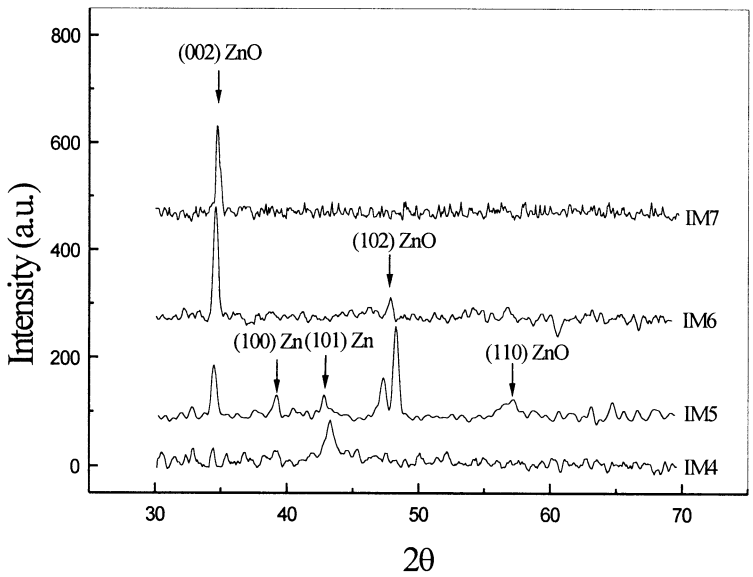

Fig. 1. XRD spectra of the samples. IM4: as-implanted; IM5: annealed at 700 °C in O_2 for 1 h; IM6: annealed at 700 °C in O_2 for 2 h; IM7: annealed at 700 °C in N_2 and O_2 for 1 h, respectively.

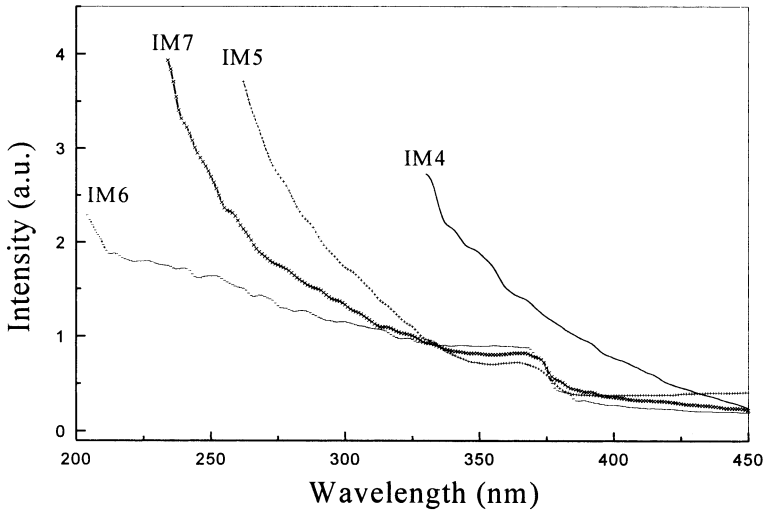

Fig. 2. Absorption spectra of the samples. IM4: as-implanted; IM5: annealed at 700 °C in O_2 for 1 h; IM6: annealed at 700 °C in O_2 for 2 h; IM7: annealed at 700 °C in N_2 and O_2 for 1 h, respectively.

The as-implanted sample, IM4, shows polycrystalline Zn with a (101) preferred orientation. As the as-implanted zinc implanted silica was annealed at 700 °C in O_2 for 1 h (IM5), some Zn atoms underwent a transformation from Zn to ZnO. The IM5 data shows mixed patterns of Zn and ZnO peaks. As the annealing time increases to 2 h, the Zn almost entirely transforms to ZnO. IM6 shows a pattern of ZnO with (002) preferred orientation and only two peaks appear (at $2\theta = 34.564$ and 47.5°) which corresponds to (002) and (102) directions of the hexagonal ZnO structure. Next, as as-implanted zinc implanted silica was annealed sequentially at 700 °C in nitrogen and then in oxygen for 1 h, respectively, the IM7 data just shows a pattern of ZnO film with (002) preferred orientation and only one peak appears (at $2\theta = 34.827°$). In terms of XRD data, the angular peak position of bulk ZnO with (002) orientation is located at $2\theta = 34.42°$ [12]. The shift of the diffraction peak from its normal bulk ZnO value is associated with the change in the lattice constant of ZnO nanoparticles. From Fig. 1, we observe the blueshift of (002) diffraction peak of IM6 and IM7 comparative to bulk ZnO. This blueshift indicated the decrease in the lattice constant parallel to *c*-axis of ZnO nanoparticles. This phenomenon can be attributed to the surface effect [13] (the large surface tension originated from the small size of nanoparticles can induce lattice distortion and decrease the lattice constant) of ZnO nanoparticles.

To evaluate the mean grain size of the samples, we used the Scherrer formula [14]:

$$D = \frac{0.9\lambda}{B\cos(\theta_B)}$$

where λ, θ_B and B are the X-ray wavelength (1.5418 Å), Bragg diffraction angle and full width at half maximum (FWHM) of (002) peak around 34.42°, (102) peak around 47.3° or (101) peak around 43.3°, respectively. The Zn mean grain size in IM4 and IM5 are 10 and 20 nm, respectively. The (002) oriented ZnO mean grain size in IM5, IM6 and IM7 are 20, 40 and 40 nm, respectively. The (102) oriented ZnO mean grain size in IM6 is 20 nm. These results indicate that Zn diffused and transformed from Zn to ZnO in the samples. Zinc implanted silica sequentially annealed at 700 °C in nitrogen and oxygen for 1 h, respectively, can create more preferred oriented ZnO nanoparticles than annealing at 700 °C in oxygen for 2 h. This result may originate from Zn reaching near the silica surface as IM7 was annealed in nitrogen ambient.

Fig. 2 shows the absorption spectra of as-implanted and annealed zinc implanted silica under different annealing conditions. These spectra were taken at room temperature. The annealed zinc implanted silica exhibit prominent exciton absorption features resulting from the relatively large binding energy of the exciton (60 meV) [15], as the annealing time increases. However, the exciton peak at 369 nm cannot be observed for as-implanted zinc implanted silica. The exciton absorption peak of the annealed sample (369 nm) is blue-shifted relative to the bulk ZnO (373 nm). Generally, the quantum confinement effect [16] and the surface effect can give rise to the blueshift of the nanoparticles energy band.

An expression for the energy band including the quantum confinement effect is given as follows [17]:

$$\mathrm{Eg} = \mathrm{Eg}_0 + \frac{\hbar^2\pi^2}{2d^2\mu} - \frac{1.8e^2}{\epsilon d},$$

where Eg_0 is the energy gap for bulk material, d the particle radius, $\mu = m_e + m_h$ (here, m_e and m_h are the effective

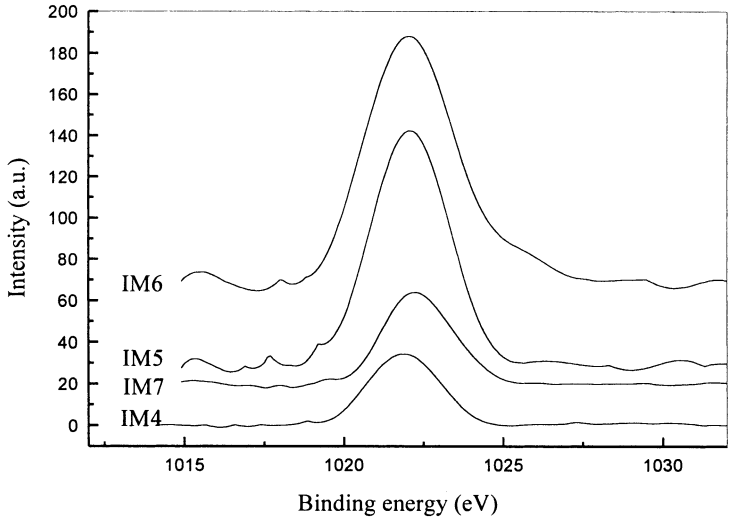

Fig. 3. XPS spectra of Zn $2P_{3/2}$ peak for zinc implanted silica under different annealing conditions. IM4: as-deposited; IM5: annealed at 700 °C in O_2 for 1 h; IM6: annealed at 700 °C in O_2 for 2 h; IM7: annealed at 700 °C in N_2 and O_2 for 1 h, respectively.

masses of the electrons and holes, respectively) and ϵ is the dielectric constant. For ZnO, the effective masses of electrons and holes are 0.24 m_0 and 0.45 m_0, respectively, and the dielectric constant is 3.7 [18]. The calculated enhanced energy band gap due to the confinement effect is about 6 meV. In fact, the exciton absorption peak of the annealed sample is blue-shifted 36 meV relative to the bulk ZnO. Therefore, we think that this blueshift mainly originate from the surface effect of ZnO nanoparticles. The absorption results are in agreement with the XRD analysis.

To identify Zn diffusion, oxidation and effusion processes during annealing process for zinc implanted silica under different annealing conditions, XPS was used to determine the chemical bonding configurations and to describe the processes of transformation from Zn to ZnO during annealing procedures.

Fig. 3 shows typical high-resolution XPS spectra from the Zn $2P_{3/2}$ core levels. The binding energy scale was calibrated using the C1s peak as reference energy (284.6 eV). According to the results of XRD and absorption spectra, the Zn $2P_{3/2}$ spectra of IM4, IM5, IM6 and IM7 can be described as the superposition of two components (Zn^0 and Zn^{+2}) peaks, corresponding to Zn atoms and ZnO nanoparticles. Fig. 4

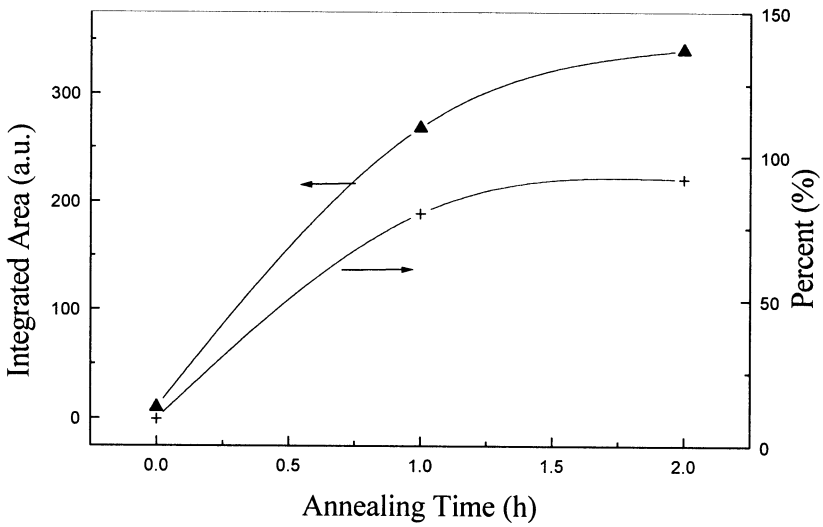

Fig. 4. The dependence of integrated area under the Zn $2P_{3/2}$ peak and the percent of oxidized Zn atoms for zinc implanted silica on the annealing time in O_2 ambient.

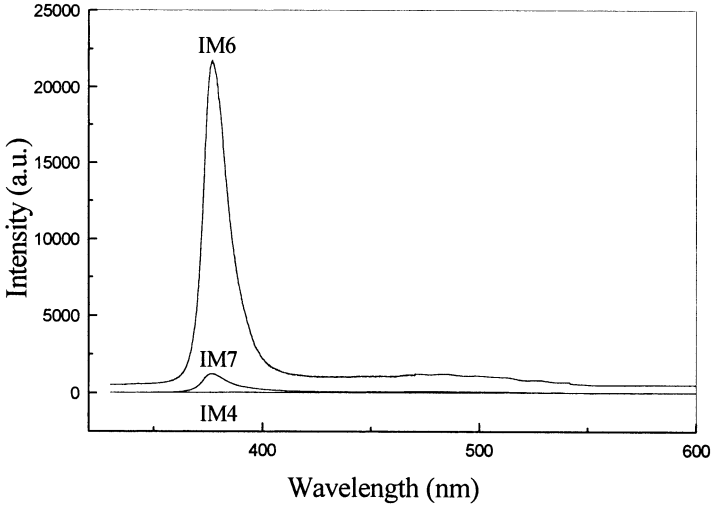

Fig. 5. Micro-PL spectra of the samples. IM4: as-implanted; IM5: annealed at 700 °C in O_2 for 1 h; IM6: annealed at 700 °C in O_2 for 2 h; IM7: annealed at 700 °C in N_2 and O_2 for 1 h, respectively.

shows the dependence of the total integrated area of Zn $2P_{3/2}$ for Zn and ZnO components and the percent of oxidized Zn atoms for annealed zinc implanted silica on the annealing time in O_2 ambient. From Fig. 4, we find that the total integrated area of Zn $2P_{3/2}$ for Zn and ZnO component and the percent of oxidized Zn atoms increase with increasing oxidation time. About 10% of Zn atoms were oxidized for as-deposited silica. As the annealing time increases to 1 h, about 78% of Zn atoms were oxidized. As the annealing time increases to 2 h, about 93% of Zn atoms were oxidized. These results are perfectly in agreement with the results of XRD spectra. Furthermore, from XPS analysis of Si $2P_{3/2}$ core level, the decrease in Si content on the silica surface with increasing annealing time was observed. Therefore, as the annealing time varies from 0 to 2 h in oxygen, the processes of Zn diffusion from inside to silica surface, Zn nucleation and Zn oxidation on silica surface occur and finally ZnO nanoparticles cover the whole silica surface. However, compared with IM6 in Fig. 3, a decrease in the integrated area of Zn $2P_{3/2}$ for IM7 was observed. IM6 and IM7 have the same annealing time and temperature. The difference is just the gas environment and oxidation time. Therefore, Zn transverse diffusion and reaching the silica surface were enhanced during annealing in nitrogen.

To investigate the ZnO nanocrystal quality and the size-distribution of ZnO nanoparticles, the micro-PL experiment was performed at room temperature. Fig. 5 shows the micro-PL spectra of zinc implanted silica annealed at 700 °C under different annealing conditions. A significant PL peak was not observed in the as-implanted sample. As zinc implanted silica was sequentially annealed in nitrogen and oxygen ambient for 1 h, the ultraviolet emission around 377 nm was obtained. As zinc implanted silica was annealed in oxygen ambient for 2 h, the ultraviolet emission around 377 nm was greatly enhanced. The FWHM of UV emission peak for IM6 and IM7 are 96 and 93 meV, respectively. This result indicated sequentially annealing zinc implanted silica in nitrogen and oxygen ambient for 1 h can create high quality ZnO nanoparticles with (002) preferred orientation and narrow size-distribution.

According to the above discussion, it appears that there are three factors to effect the transformation from Zn to ZnO during the annealing processes of zinc implanted silica. They are the annealing temperature, the time and the gas environment. The annealing temperature and time determine the content of the surface Zn atoms due to Zn diffusion from inside to the surface and Zn effusion on silica surface. The annealing time and gas environment determine the degree of the oxidation of the surface Zn atoms. Based on our experimental results, the annealing temperature of 700 °C is higher than the Zn melting point. So Zn diffusion was enhanced.

From Fig. 4, we observe that Zn atoms near the silica surface almost transformed entirely to ZnO as the annealing time increased to 2 h.

Tomlins et al. have reported that the Zn diffusion coefficient along the *a*-axis direction is the same as that along *c*-axis direction [19]. For as-deposited zinc implanted silica, the Zn ions distribution forms a Gaussian shape in silica along *c*-axis direction. This distribution can give rise to the anisotropy of Zn diffusion in silica and enhance the Zn diffusion along *c*-axis direction. Therefore, as the annealing time increases, Zn atoms inside silica diffuse to the silica surface, nucleate resulting from transverse diffusion on the silica surface and oxidize easily in oxygen due to the uniform distribution of Zn atoms on silica surface after annealing in nitrogen. We also sequentially annealed zinc implanted silica at 900 °C in nitrogen and oxygen for 1 h, respectively. However, the XRD and absorption spectra do not show the formation of ZnO nanoparticles. We can just

observe the formation of a thin uniform blue film on the surface of silica with the naked eye. This result is in agreement with the fact that Zn transverse diffusion near silica surface and Zn effusion on silica surface are enhanced as the annealing temperature increases. In our opinion, post-thermal sequentially annealing zinc implanted silica in nitrogen and oxygen ambient, respectively, is a good method for obtaining high quality ZnO nanoparticles with (002) preferred orientation and narrow size-distribution.

4. Conclusions

The dynamic processes of ZnO nanoparticles formed by post-thermal annealing zinc implanted silica were investigated by XRD, absorption, XPS and micro-PL spectra. As-implanted zinc implanted silica contains Zn nanoparticles with (101) orientation. Zinc implanted silica was annealed at 700 °C in oxygen for 2 h, and sequentially in nitrogen and oxygen for 1 h, respectively. The two methods can yield ZnO nanoparticles with (002) preferred orientation, however, the latter method creates high ZnO nanoparticles with (002) preferred orientation and narrow size-distribution due to Zn transverse diffusion near silica surface and Zn effusion on silica surface after annealing in nitrogen.

Acknowledgements

This work was supported by the Program of CAS Hundred Talents, the National Fundamental and Applied Research Project, the National Natural Science Foundation of China, the Key Project of the National Natural Science Foundation of China (No. 69896260), the Key Project of the Science and Technology from Ministry of Education of China and Jilin Distinguished Young Scholar Program.

References

[1] T. Mitsuyu, S. One, K. Wesa, J. Appl. Phys. 51 (1980) 2464.
[2] D.M. Bagnall, Y.F. Chen, Z. Zhu, T. Yao, M.Y. Shen, T. Goto, Appl. Phys. Lett. 73 (1998) 1038.
[3] P. Yu, Z.K. Tang, G.K.L. Wong, M. Kawasaki, A. Ohtomo, H. Koinuma, Y. Segawa, J. Cryst. Growth 184/185 (1998) 601.
[4] J.G.E. Gardeniers, Z.M. Rittersma, G.J. Burger, J. Appl. Phys. 83 (1998) 7844.
[5] Y. Chen, D.M. Bagnall, H.J. Koh, K.T. Park, K. Hiraga, Z. Zhu, T. Yao, J. Appl. Phys. 84 (1998) 3912.
[6] S. Bethke, H. Pan, B.W. Wesseis, Appl. Phys. Lett. 52 (1988) 138.
[7] R.D. Vispute, V. Talyansky, S. Choopun, R.P. Sharma, T. Venkatesan, M. He, X. Tang, J.B. Halpern, M.G. Spencer, Y.X. Li, K.A. Jones, Appl. Phys. Lett. 73 (1998) 348.
[8] H. Nanto, T. Minami, S. Takata, Phys. Status Solidi A 65 (1981) k131.
[9] F. Paraguay, D.W. Estrada, D.R. Acosta, N.E. Andrade, M. Miki-Yoshida, Thin Solid Films 350 (1999) 192.
[10] S. Cho, J. Ma, Y. Kim, Y. Sun, G.K.L. Wang, J.B. Ketterson, Appl. Phys. Lett. 75 (1999) 2761.
[11] R. Mu, D.O. Henderson, Y.S. Tung, A. Ueda, C. Hall, W.E. Collins, C.W. White, R.A. Zuhr, J.G. Zhu, J. Vac. Sci. Technol., A 14 (3) (1996) 1482.
[12] V. Gupta, A. Mansingh, J. Appl. Phys. 80 (1996) 1063.
[13] Z. Lide, M. Jimei, Nanomater. Nanostruct. 81 (2001) in Chinese.
[14] B.D. Cullity, Elements of X-ray of Diffractions, Addison-Wesley, Reading, MA, 1978 P102.
[15] Z.K. Tang, G.K.L. Wong, P. Yu, M. Kawasaki, A. Ohtomo, H. Konuma, Y. Segawa, Appl. Phys. Lett. 72 (1998) 3270.
[16] M. Haase, H. Weller, A. Henglein, J. Phys. Chem. 92 (1988) 482.
[17] L. Brus, J. Chem. Phys. 80 (1984) 4403.
[18] E.M. Wong, P.C. Searson, Appl. Phys. Lett. 74 (1999) 2939.
[19] G.W. Tomlins, J.L. Routbort, T.O. Mason, J. Appl. Phys. 87 (2000) 117.